Experimental Generation of Robust Entanglement from Classical Correlations via Local Dissipation

Adeline Orieux,[1,*] Mario A. Ciampini,[1] Paolo Mataloni,[1,2] Dagmar Bruß,[3] Matteo Rossi,[4] and Chiara Macchiavello[4]
[1]Dipartimento di Fisica, Sapienza Università di Roma, Piazzale Aldo Moro, 5, I-00185 Roma, Italy
[2]Istituto Nazionale di Ottica, Consiglio Nazionale delle Ricerche (INO-CNR), Largo Enrico Fermi, 6, I-50125 Firenze, Italy
[3]Institut für Theoretische Physik III, Heinrich-Heine-Universität Düsseldorf, D-40225 Düsseldorf, Germany
[4]Dipartimento di Fisica and INFN-Sezione di Pavia, via Bassi 6, I-27100 Pavia, Italy
(Received 17 March 2015; revised manuscript received 2 June 2015; published 16 October 2015)

We experimentally show how classical correlations can be turned into quantum entanglement, via the presence of dissipation and the action of a CNOT gate. We first implement a simple two-qubit protocol in which entanglement production is not possible in the absence of such kind of noise, while it arises with its introduction, and is proportional to its amount. We then perform a more elaborate four-qubit experiment, by employing two hyperentangled photons initially carrying only classical correlations. We demonstrate a scheme where the entanglement is generated via local dissipation, with the advantage of being robust against local unitaries performed by an adversary.

DOI: 10.1103/PhysRevLett.115.160503 PACS numbers: 03.67.Bg, 42.50.Dv, 42.50.Ex

Introduction.—Entanglement is the most precious resource in quantum information processing [1,2]. However, what is most precious is often also most fragile. Indeed, a profound opponent of entanglement is noise: decoherence and dissipation both typically decrease entanglement, unless they are tailored specifically in a collective way, such as, for example, in correlated noisy channels [3,4], or in engineered dissipation of coupled systems [5] or in the presence of tunable noise [6]. Hence, in general, except for peculiar experimental conditions, noise represents a strong obstacle for entanglement.

In this work we introduce a scenario where, with fixed given resources of input states and gates, no entanglement can be produced, unless one switches on *any* local nonunital noise, such as dissipation. Note that not all types of noise would work: for instance dephasing, which is unital, would not be helpful here. In this setting entanglement is zero without noise, and it grows with the amount of the introduced local noise. An important aspect of this quantum effect is the choice of the dimension of the underlying Hilbert space: as long as only two qubits are present, we will show that an adversary (Eve) is always able to prevent the production of entanglement by applying a suitable local rotation. We will also show that, however, by embedding the protocol into a higher-dimensional Hilbert space, concretely by using four qubits, the creation of entanglement via local noise can be made robust against any possible unitary action of Eve. Interestingly, in order to achieve this robustness it is sufficient to have input states that exhibit just classical correlations. Experimentally, the different dimensional settings of two and four qubits are implemented using the path and polarization degrees of freedom of photons and the fragility of the effect in low dimensions is demonstrated.

The reason behind this effect is an intricate relationship between the concepts of separability, quantum correlations, and entanglement: a necessary ingredient for the production of entanglement in our scenario is the generation of nonvanishing off-diagonal terms ("quantum coherences") in the initial density matrix, which may arise via a local nonunital channel. However, the presence of quantum coherences is not sufficient for robustness of the protocol, in the sense explained above. A sufficient ingredient for robustness is the presence of classical correlations within the initial state: they are turned into correlations of a quantum nature (often referred to as "discord") via a local nonunital channel, which still keeps the quantum state separable. Finally, the quantum correlations are activated into nonvanishing entanglement with a CNOT gate.

Generation of quantum correlations from classical correlations by local noise was theoretically investigated in Ref. [7], see also Refs. [8,9], and experimentally demonstrated with trapped ions [10], while entanglement activation from discord was theoretically proposed in Ref. [11] (for a different interpretation see Ref. [12]), and experimentally demonstrated in Ref. [13]. In the scenario that we propose here these two effects are combined, resulting in a scheme where we are able to generate entanglement in a robust way, starting from classically correlated states at the input and switching on a local noisy device, acting on a single qubit.

Theory.—Let us briefly describe the fixed resources for the two-qubit scheme [see Fig. 1(a)]: we are given two qubits in a product state, where a qubit is in the maximally mixed state $\rho_A = \frac{\mathbb{1}}{2}$ and an ancilla is in the state $\rho_C = |0\rangle\langle 0|$. We are also given a CNOT gate with $A(C)$ the control (target) qubit and we are allowed to perform any possible local unitary operation on A and C. The goal is to create

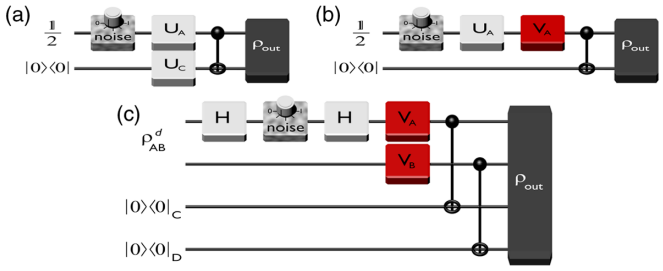

FIG. 1 (color online). (a) Two-qubit scheme: the entangled output state ρ_{out} is generated by starting from the initial state $\frac{\mathbb{I}}{2} \otimes |0\rangle\langle 0|$, and using local unitaries U_A and U_C and a CNOT gate. A local nonunital noisy element can be switched on by turning the knob. (b) The same protocol in the presence of an adversary player using a local unitary V_A to try and prevent the generation of entanglement. (c) Four-qubit scheme: here ρ^d_{AB} represents a bipartite state, diagonal in the computational basis, with the same block of gates defined in the two-qubit scenario. The aim is to switch on entanglement of ρ_{out} with respect to the cut $AB|CD$ by exploiting local noise.

entanglement in the total state ρ_{out} of qubits A and C. It is clear that with only these fixed resources at our disposal it is not possible to create entanglement in the bipartite system considered here.

If in addition we are allowed to use a local noisy device acting only on qubit A, such as an amplitude damping channel (see later for details), as reported in Fig. 1(a), the situation changes. Even if at first glance we might expect that our ability to generate entanglement could not be improved by adding such a resource, since the operation is local and noisy channels are usually regarded as detrimental for quantum features, it turns out that if this extra resource is nonunital (i.e., if it does not preserve the identity) it allows us to produce an entangled output state ρ_{out}. Indeed, if ρ_A is not the identity anymore, off-diagonal elements can appear in it after the application of a unitary U_A, resulting in entanglement in ρ_{out} after the CNOT gate. One can also show that the generation of entanglement in this protocol can always be prevented by a suitable local rotation (that makes ρ_A diagonal again) performed by some adversary before the action of the CNOT gate, as shown in Fig. 1(b). Note that in this two-qubit scenario, no classical correlations are present in the initial state; thus, no quantum correlations are created by the nonunital channel, which is why the entanglement activation is not robust [13].

We will now present a four-qubit scheme where the entanglement will not be vulnerable anymore to local rotations. We begin with a two-qubit state ρ^d_{AB}, which is diagonal in the computational basis (which is a factorized basis) and therefore exhibits at most classical correlations, and two ancilla qubits C and D, both initialized in the state $|0\rangle\langle 0|$. We can then apply two CNOT gates operating on qubits AC and BD [see Fig. 1(c) with the noisy device switched off]. Under these conditions the output state will always be a separable state [11].

We now introduce a local nonunital noisy device, acting on qubit A, given by the block of gates $H\Lambda_\eta H$, where H is the Hadamard transform and Λ_η is an amplitude damping channel, where the noise parameter η can be tuned by a knob. Its action is explicitly described by $\Lambda_\eta(\rho) = \sum_{i=1}^{2} A_i^\dagger \rho A_i$, with the Kraus operators $A_1 = |0\rangle\langle 0| + \sqrt{1-\eta}|1\rangle\langle 1|$, $A_2 = \sqrt{\eta}|0\rangle\langle 1|$ with $\eta \in [0,1]$, where $\eta = 0$ corresponds to the noiseless case. Note that this channel is a model for dissipation.

We show in the following that by adding only this extra local noisy resource entanglement is switched on at the output of the circuit in the bipartition $AB|CD$, starting from input states which are at most classically correlated. Such states read

$$\rho_{\text{in}} = [p|00\rangle\langle 00| + (1-p)|11\rangle\langle 11|]_{AB} \otimes |00\rangle\langle 00|_{CD}. \tag{1}$$

They are transformed by the circuit of Fig. 1(c) into block-diagonal output states:

$$\rho_{\text{out}} = p\rho^+_{AC} \otimes |00\rangle\langle 00|_{BD} + (1-p)\rho^-_{AC} \otimes |11\rangle\langle 11|_{BD}. \tag{2}$$

Here we have defined

$$\rho^\pm = \frac{1}{2}[(1 \pm \sqrt{\bar{\eta}})|00\rangle\langle 00| + (1 \mp \sqrt{\bar{\eta}})|11\rangle\langle 11| + \eta(|00\rangle\langle 11| + |11\rangle\langle 00|)] \tag{3}$$

with $\bar{\eta} = 1 - \eta$. In order to quantify the entanglement of ρ_{out} with respect to the splitting $AB|CD$, we apply the partial transposition T_{AB} with respect to AB, and study the negative eigenvalues of $\rho_{\text{out}}^{T_{AB}}$. For $\eta \neq 0$ there are two negative eigenvalues, namely, $\lambda_1^- = -p(\eta/2)$ and $\lambda_2^- = -(1-p)\eta/2$. We quantify the amount of entanglement in terms of the negativity, defined as $N(\rho) = \sum_i |\lambda_i^-|$. Thus, for any state ρ_{in} as in Eq. (1) the negativity of the output state as in Eq. (2) is given by

$$N(\rho_{\text{out}}) = \frac{\eta}{2}. \tag{4}$$

Therefore, the entanglement increases linearly by increasing the noise parameter. Note that the negativity in Eq. (4) is independent of p; however, the amount of classical correlations in the initial state is not. Indeed, in this four-qubit scheme, an adversary using two local unitaries V_A and V_B just before the CNOT gates cannot prevent the presence of entanglement in ρ_{out} as long as classical correlations are present in the initial state ($p \neq 0, 1$) and as long as they are transformed into discord by the nonunital channel ($\eta \neq 0, 1$).—Theoretical details of the different robustness properties of both protocols are reported in the Supplemental Material [14].

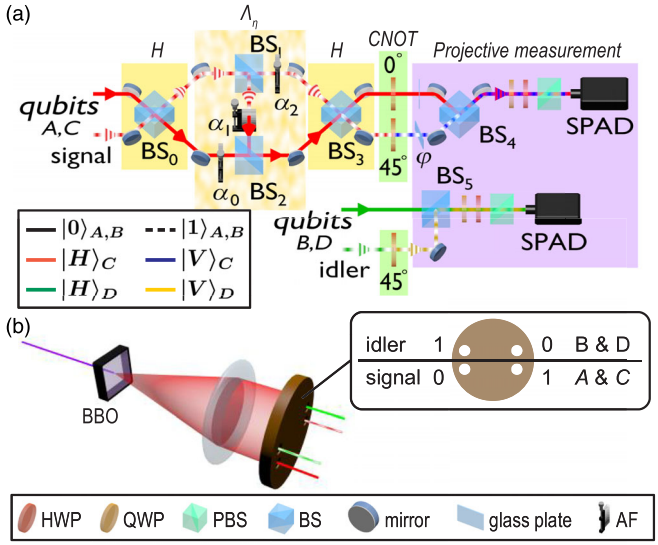

FIG. 2 (color online). (a) Experimental setup for the four-qubit protocol (the two-qubit experiment employs the same apparatus with the CNOT on the idler photon removed: this photon serves only as trigger). BSs: balanced beam splitters, BS_0 and BS_3 implement the Hadamard gates H; BS_1 and BS_2, together with the tunable attenuation filters α_0, α_1 and α_2, constitute the amplitude damping channel Λ_η. Path analysis of photons is performed through the phase plate φ and BS_4, BS_5. Polarization analysis is performed through a standard polarization tomography setup. PBS: polarizing beam splitter, HWP (QWP): half-(quarter-)wave plate. SPAD: single photon avalanche photodiode. Eve's attack is simulated by removing BS_3. (b) SPDC source. A cw 355 nm pump is injected into a type I BBO crystal, generating 710 nm correlated photon pairs through SPDC. A 4-hole mask selects path qubits; qubit A (B) is encoded in the path of the signal (idler) photon, qubit C (D) is encoded in the polarization of the signal (idler) photon.

Experiment: two-qubit protocol.—The two-qubit protocol was implemented with the optical setup shown in Fig. 2(a) where qubits A and C (encoded, respectively, in the path and the polarization degrees of freedom (DOFs) of the signal photon) were used. Note that the actual setup consisted in a folded version (a Sagnac configuration), which guarantees an intrinsic phase stability for the path qubits. Horizontally polarized degenerate photon pairs [see Fig. 2(b)] are emitted by spontaneous parametric down-conversion (SPDC) on the surface of a cone, two photons of the same pair being diametrically opposite [16]. A 4-hole mask intercepted the emission cone, selecting the two pairs of modes $|00\rangle\langle 00|_{\text{signal,idler}}$ or $|11\rangle\langle 11|_{\text{signal,idler}}$. In this configuration, the source naturally generates a path-entangled Bell state. In order to ensure that only classical correlations are present in the input state for the experiments at hand, the phase coherence between these two possible pairs is destroyed by having an optical path difference between any two path modes larger than the photon's coherence time. Thus, the input state was prepared with the path qubit in the state $\rho_A^d = \frac{1}{2}(|0\rangle\langle 0|_A + |1\rangle\langle 1|_A)$, and the polarization qubit was in the state $|H\rangle\langle H|_C$, where $H(V)$ designs the horizontal (vertical) polarization and corresponds to the state 0 (1) of the computational basis.

Both Hadamard gates H were realized with balanced beam splitters (BSs). The amplitude damping channel Λ_η was achieved by a combination of two BSs (BS_1 and BS_2) and three attenuation filters allowing us to transfer, in a tunable way, a portion of mode $|1\rangle$ onto mode $|0\rangle$ of the path qubit A. The relationship between the noise parameter η and the intensity transmission coefficients α_0, α_1, and α_2 of the attenuators is (see calculation in the Supplemental Material [14]): $\alpha_0 = R^2/T = 31\%$, $\alpha_1 = \eta$ and $\alpha_2 = \alpha_0(1-\eta) = R^2/T(1-\eta)$, with $T = 57.5\%$ ($R = 42.5\%$) the measured intensity transmission (reflection) coefficient of the BSs. For each setting of η, the transmission of each attenuator was tuned to these values by adjusting their position relative to the beam. The CNOT gate was implemented by inserting a half-wave plate (HWP) at 45° in the path mode corresponding to $|1\rangle_A$. A HWP at 0° was also inserted in the other path mode to maintain the same optical length for both modes.

Finally, the entanglement in the output state of AC was estimated by a standard tomographic reconstruction measurement of the two-qubit state [17] from which we recovered the negativity N: in Fig. 3(a) we report its measured value obtained for different values of η (blue squares), together with its theoretical value given by Eq. (4) (dark line). The dashed blue line corresponds to the expected theoretical value, taking into account the finite interference visibility achieved in the interferometers (see Supplemental Material [14]). The figure shows a good agreement between the measured and theoretical behaviors, demonstrating that the amount of entanglement created increases with the noise. The deviation from the theoretical behavior, in the experimental value of N for $\eta = 0.5$ in Fig. 3(a), is caused by an unexpected discontinuity in the attenuator α_1.

As expected, the creation of entanglement can be prevented by Eve for any amount of noise. With the protocol of Fig. 1(b) the best strategy for Eve is to perform another Hadamard gate ($V_A = H_{\text{Eve}}$) to cancel the action of the second Hadamard. Indeed, in this way, even though the noise is nonunital, the density matrix of qubit A remains diagonal (in the computational basis), so no entanglement is generated. In order to simulate Eve's attack experimentally we simply removed BS_3 from our setup (see Fig. 2). As expected, the negativity measured in this case is always vanishing [see Fig. 3(a), red crosses].

Experiment: four-qubit protocol.—We then implemented the four-qubit scheme shown in Fig. 2(a): two extra qubits B and D, encoded respectively in the path and the polarization DOFs of the idler photon, were added. The prepared input state was $\rho_{AB}^d = p|00\rangle\langle 00|_{AB} + (1-p)|11\rangle\langle 11|_{AB}$, with $p \simeq 0.5$ for the path qubits, and

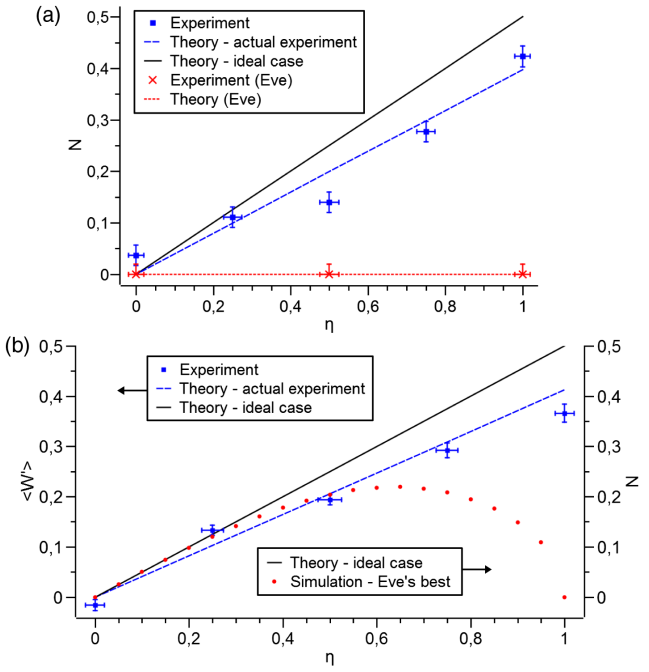

FIG. 3 (color online). Experimental results. (a) Two-qubit protocol: negativity $N(\rho_{\text{out}})$ vs the noise parameter η. (b) Four-qubit protocol: expectation value $\langle W' \rangle = -\langle W \rangle$ of the entanglement witness applied to ρ_{out} as a function of η. The dashed lines correspond to a theoretical calculation that takes into account the actual experimental apparatus. The red dots represent the adversary's best strategy. In the four-qubit case they report a simulation of the minimal amount of entanglement (quantified by N) that can be generated after the application of local rotations on qubits A and B by an adversary. Error bars are calculated from photon counting statistics (see Supplemental Material [14]).

$|H\rangle\langle H|_{C,D}$ for both polarization qubits. All the gates were implemented as in the two-qubit setup. The additional CNOT gate between qubits B and D was implemented by a HWP at 45° in the path mode $|1\rangle_B$.

We checked for entanglement in the splitting $AB|CD$ by using the entanglement witness

$$W = \frac{1}{8}(\mathbb{1} \otimes \mathbb{1} - \sigma_x \otimes \sigma_x + \sigma_y \otimes \sigma_y - \sigma_z \otimes \sigma_z)_{AC} \otimes (\mathbb{1} \otimes \mathbb{1} + \sigma_z \otimes \sigma_z)_{BD}, \quad (5)$$

where σ_x, σ_y and σ_z are the Pauli matrices. This witness certifies the presence of bipartite entanglement in the final state ρ_{out}, whenever $\langle W \rangle < 0$ [18]. It was constructed as follows: the eigenvectors of $\rho_{\text{out}}^{T_{AB}}$, see Eq. (2), are $|\lambda_1^-\rangle = |\Psi^-\rangle_{AC} \otimes |00\rangle_{BD}$ and $|\lambda_2^-\rangle = |\Psi^-\rangle_{AC} \otimes |11\rangle_{BD}$, with $|\Psi^-\rangle = 1/\sqrt{2}(|01\rangle - |10\rangle)$; therefore, an entanglement witness with respect to the splitting $AB|CD$ can be defined as $W = (|\lambda_1^-\rangle\langle\lambda_1^-| + |\lambda_2^-\rangle\langle\lambda_2^-|)^{T_{AB}}$, which, if decomposed in terms of local operators, takes the form Eq. (5). Notice that the experimental detection of W requires only the three measurement settings $\{\sigma_x\sigma_z\sigma_x\sigma_z, \sigma_y\sigma_z\sigma_y\sigma_z, \sigma_z\sigma_z\sigma_z\sigma_z\}$ (in lexicographic order $ABCD$) that reduced to 32 projective measurements (see Eq. S15 in the Supplemental Material [14]). Pauli operations on qubits A and B were performed by a standard polarization analysis setup, while qubits C and D were analyzed by selecting proper phase values between BS_3 and BS_4 [see Fig. 2(a)].

In Fig. 3(b) we show the measured expectation value $\langle W' \rangle = -\langle W \rangle$ of the witness as a function of η (blue squares). This quantity provides a lower bound for the negativity of ρ_{out}: $N(\rho_{\text{out}}) \geq \langle W' \rangle$ [19]. The blue dashed line corresponds to the theoretical evolution computed with the experimental imperfections and the measured value of p in the input state (see the Supplemental Material [14]). Our results are in agreement with Eq. (4): while there is no entanglement when local noise is absent ($\eta = 0$), it is generated as the noise increases. The experimental demonstration of the robustness of the protocol would require the actual measurement of a nonvanishing entanglement measure for every possible unitary operation that Eve can apply on qubits A and B. As this is not practically feasible in our setup, instead we numerically computed the minimal amount of entanglement that is generated by the protocol when Eve adopts the local rotations on qubits A and B that best reduce this entanglement. This result [see red dots in Fig. 3(b)] is obtained, for each value of η, by a minimization of the negativity over all possible unitaries V_A and V_B. Notice that when the noise level is low, i.e., η is close to zero, Eve's best attack cannot reduce much the amount of created entanglement. Only in the extreme cases $\eta = 0, 1$ she can totally prevent the creation of an entangled output state.

Conclusion.—We have shown that quantum entanglement can be switched on by the help of a local noisy device, and increases with the amount of noise introduced on purpose. Using a single photon, we experimentally created entanglement between its path and polarization degrees of freedom, demonstrating the idea in terms of a simple two-qubit protocol. A more sophisticated four-qubit scenario had the advantage over the previous one of being robust against local unitaries performed by an adversary player thanks to the initial presence of classical correlations. Our experiments have thus implemented some subtle features of the quantum world: while, obviously, no local action can produce correlations, a local nonunital quantum channel can turn classical correlations into quantum correlations [7]. The local amplitude damping channel (as a model for dissipation) that we realized performed this task, while preserving separability of the state. The quantum correlations were then activated into entanglement [11], by nonlocal gates. We emphasize that without this dissipative channel no entanglement could have been produced, and that its robustness crucially depends on the underlying Hilbert space dimension.

This work was supported by the European Union through the project FP7-ICT-2011-9-600838 (QWAD Quantum Waveguides Application and Development; www.qwad-project.eu).

*Present address: Télécom ParisTech, CNRS-LTCI, 46 rue Barrault, F-75634 Paris Cedex 13, France.
adeline.orieux@gmail.com

[1] M. A. Nielsen and I. L. Chuang, *Quantum computation and quantum information* (Cambridge University Press, Cambridge, England, 2010).
[2] D. Bruß and G. Leuchs, Lectures on Quantum Information (Wiley-VCH Verlag GmbH & Co. KGaA, Weinheim, 2007).
[3] C. Macchiavello and G. M. Palma, Phys. Rev. A **65**, 050301 (R) (2002).
[4] Y. Yeo, Phys. Rev. A **78**, 022334 (2008).
[5] H. Krauter, C. A. Muschik, K. Jensen, W. Wasilewski, J. M. Petersen, J. I. Cirac, and E. S. Polzik, Phys. Rev. Lett. **107**, 080503 (2011).
[6] M. B. Plenio and S. F. Huelga, Phys. Rev. Lett. **88**, 197901 (2002).
[7] A. Streltsov, H. Kampermann, and D. Bruß, Phys. Rev. Lett. **107**, 170502 (2011).
[8] F. Ciccarello and V. Giovannetti, Phys. Rev. A **85**, 010102 (R) (2012).
[9] X. Hu, H. Fan, D. L. Zhou, and W. M. Liu, Phys. Rev. A **85**, 032102 (2012).
[10] B. P. Lanyon, P. Jurcevic, C. Hempel, M. Gessner, V. Vedral, R. Blatt, and C. F. Roos, Phys. Rev. Lett. **111**, 100504 (2013).
[11] M. Piani, S. Gharibian, G. Adesso, J. Calsamiglia, P. Horodecki, and A. Winter, Phys. Rev. Lett. **106**, 220403 (2011).
[12] A. Streltsov, H. Kampermann, and D. Bruß, Phys. Rev. Lett. **106**, 160401 (2011).
[13] G. Adesso, V. D'Ambrosio, E. Nagali, M. Piani, and F. Sciarrino, Phys. Rev. Lett. **112**, 140501 (2014).
[14] See Supplemental Material at http://link.aps.org/supplemental/10.1103/PhysRevLett.115.160503 for further theoretical and experimental details, which includes Ref. [15].
[15] G. Vidal and R. F. Werner, Phys. Rev. A **65**, 032314 (2002).
[16] M. Barbieri, C. Cinelli, P. Mataloni, and F. De Martini, Phys. Rev. A **72**, 052110 (2005).
[17] D. F. V. James, P. G. Kwiat, W. J. Munro, and A. G. White, Phys. Rev. A **64**, 052312 (2001).
[18] O. Gühne, P. Hyllus, D. Bruß, A. Ekert, M. Lewenstein, C. Macchiavello, and A. Sanpera, Phys. Rev. A **66**, 062305 (2002).
[19] F. G. S. L. Brandao, Phys. Rev. A **72**, 022310 (2005).